Heterozygous Loss-of-Function Mutations in *YAP1* Cause Both Isolated and Syndromic Optic Fissure Closure Defects

Kathleen A. Williamson,[1,8] Joe Rainger,[1,8] James A.B. Floyd,[2] Morad Ansari,[1] Alison Meynert,[1] Kishan V. Aldridge,[1] Jacqueline K. Rainger,[1] Carl A. Anderson,[2] Anthony T. Moore,[3,7] Matthew E. Hurles,[2] Angus Clarke,[4] Veronica van Heyningen,[1] Alain Verloes,[5] Martin S. Taylor,[1] Andrew O.M. Wilkie,[6] UK10K Consortium, and David R. FitzPatrick[1,*]

Exome sequence analysis of affected individuals from two families with autosomal-dominant inheritance of coloboma identified two different cosegregating heterozygous nonsense mutations (c.370C>T [p.Arg124*] and c. 1066G>T [p.Glu356*]) in *YAP1*. The phenotypes of the affected families differed in that one included no extraocular features and the other manifested with highly variable multisystem involvement, including hearing loss, intellectual disability, hematuria, and orofacial clefting. A combined LOD score of 4.2 was obtained for the association between *YAP1* loss-of-function mutations and the phenotype in these families. *YAP1* encodes an effector of the HIPPO-pathway-induced growth response, and whole-mount in situ hybridization in mouse embryos has shown that *Yap1* is strongly expressed in the eye, brain, and fusing facial processes. RT-PCR showed that an alternative transcription start site (TSS) in intron 1 of *YAP1* and *Yap1* is widely used in human and mouse development, respectively. Transcripts from the alternative TSS are predicted to initiate at codon Met179 relative to the canonical transcript (RefSeq NM_001130145). In these alternative transcripts, the c.370C>T mutation in family 1305 is within the 5′ UTR and cannot result in nonsense-mediated decay (NMD). The c. 1066G>T mutation in family 132 should result in NMD in transcripts from either TSS. Amelioration of the phenotype by the alternative transcripts provides a plausible explanation for the phenotypic differences between the families.

Occurring in ~1 in 5,000 live births,[1] ocular coloboma is the most common major eye malformation and is typically due to an optic fissure closure defect (OFCD) during development.[2] The clinical impact of an OFCD is strongly correlated with the extent and location of the closure defect in an individual.[3] Small optic nerve and choroidoretinal OFCDs (not involving the macula) can be asymptomatic and can be discovered on investigation of apparently unaffected parents of severely affected children.[1] OFCDs involving only the iris typically present as inferonasal "keyhole" defects, which can be of cosmetic significance and cause intolerance of bright light. However, bilateral OFCDs might be a significant cause of visual impairment during childhood as a result of associated severe microphthalmia, failure of macula development, and/or retinal detachment.[4]

Segregation analysis in families has indicated that there is a strong genetic component to both bilateral and unilateral OFCDs.[1] In most individuals with an OFCD, the genetic basis of the malformation is not known. Mutations in OFCD cases have been identified in genes more commonly associated with bilateral anophthalmia (*SOX2* [MIM 184429],[5,6] *OTX2* [MIM 600037],[7] *STRA6* [MIM 610745][8]), holoprosencephaly (MIM 142945) (*SHH* [MIM 600725][9]), or aniridia (MIM 102210) (*PAX6* [MIM 607108][10,11]). OFCDs can also be a component of many different multisystem developmental syndromes, such as CHARGE syndrome (MIM 214800, caused by mutations in *CHD7* [MIM 608892]; see GeneReviews in Web Resources) and Baraitser-Winter syndrome (MIM 243310, caused by mutations in *ACTB1* [MIM 102630] and *ACTG1* [MIM 102560][12,13]). Recently, *ABCB6* (MIM 605452) was identified as a strong candidate gene via positional cloning in a large Chinese family affected by autosomal-dominant OFCDs.[14]

As part of the rare-disease component of the UK10K project, whole-exome sequencing was performed on an affected uncle-niece pair with bilateral OFCDs (Figure 1, family 1305 individuals II:2 and III:1; clinical examination by A.V.). This study was approved by the UK Multiregional Ethics Committee (reference 06/MRE00/76), and informed consent was obtained from the participating families. Exome sequencing was performed as previously described.[15] Sequences were aligned with the Burrows-Wheeler Aligner v.0.5.9, duplicates were marked with Picard v.1.43, indels were realigned and base quality scores were recalibrated with the Genome Analysis Toolkit (GATK) v.1.0.5506, and variants were called only with the GATK Unified Genotyper. The shared variant filtering in this family is summarized in Table 1. No significant

[1]Medical Research Council Human Genetics Unit, Medical Research Council Institute of Genetics and Molecular Medicine, University of Edinburgh, Edinburgh EH4 2XU, UK; [2]Wellcome Trust Sanger Institute, Genome Campus, Hinxton, Cambridgeshire CB10 1SA, UK; [3]Moorfields Eye Hospital NHS Foundation Trust, London EC1V 2PD, UK; [4]Institute of Medical Genetics, University Hospital of Wales, Cardiff CF14 4XW, UK; [5]Département de Génétique, Hôpital Robert-Debré, 75019 Paris, France; [6]Weatherall Institute of Molecular Medicine, John Radcliffe Hospital, University of Oxford, Oxford OX3 9DS, UK; [7]University College London Institute of Ophthalmology, London EC1V 9EL, UK
[8]These authors contributed equally to this work
*Correspondence: david.fitzpatrick@igmm.ed.ac.uk
http://dx.doi.org/10.1016/j.ajhg.2014.01.001.

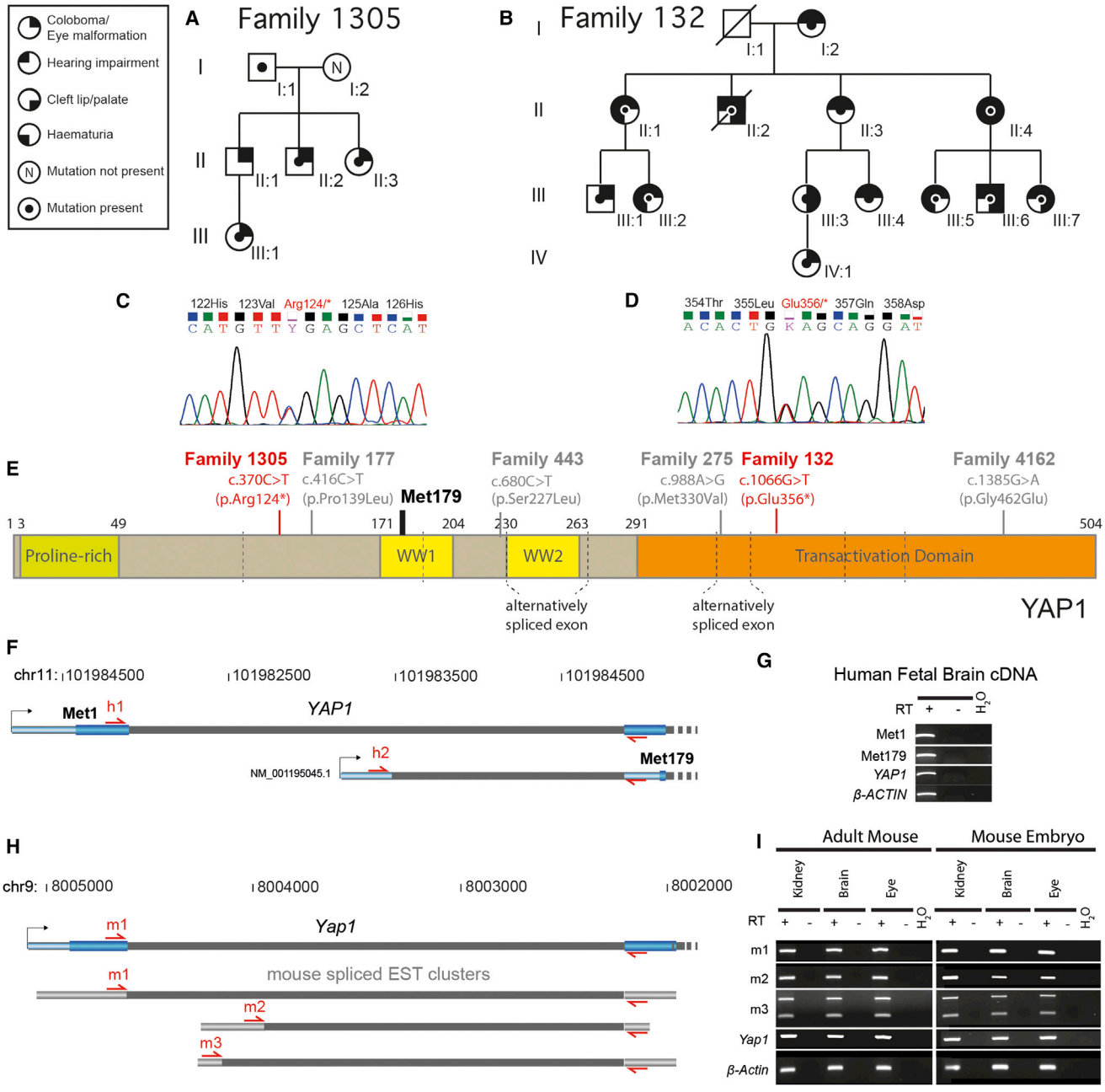

Figure 1. Position and Consequences of *YAP1* Mutations

(A) Pedigree structure of family 1305 (F1305). The symbol key is shown on the left. DNA was available from three affected (II:2, II:3, and III:1) and two unaffected (I:1 and I:2) individuals.

(B) An abridged version of the published pedigree of family 132 (F132, Ravine et al.[17]) shows affected individuals from whom DNA samples were available.

(C and D) Representative chromatograms of the confirmatory Sanger sequencing that was performed in all individuals from whom DNA was available in families 1305 and 132.

(E) A diagram of the domain structure of YAP1. The amino acid numbers indicating the beginning and end of each domain are shown above relative to isoform 1 (P46937, UniProt). The positions of the exon junctions are indicated by the vertical gray dashed lines. The positions of the nonsense mutations are shown in red text, and the probably nonpathogenic missense mutations are shown in gray text. The probable initiating methionine used in transcripts from the alternative transcription start site (TSS) is indicated by Met179.

(F and H) Diagrams of the 5′ end of the gene models for the canonical and alternative TSSs in human and mouse, respectively. In both species, the most 5′ TSS is canonical and encodes transcripts with an open reading frame that uses the initiation methionine Met1. The TSS in intron 1 of the canonical transcript splices to the same exon 2, but in this transcript, the initiating methionine is equivalent to Met179 of the canonical transcript.

(G and I) A gel photograph shows the results of RT-PCR using primers indicated by the red arrows on the cognate gene models and the tissues indicated above each lane. This shows that the alternative TSS was present in all examined tissues.

Table 1. Shared Variant Filtering for Family 1305

	Family 1305	
	Uncle (II:2)	**Niece (III:1)**
VCF code	COL5103588	COL5103589
Average depth	36.6	36.5
Total number of variant calls	101,283	104,337
Number of variants passing quality filters	42,822	43,786
Number of variants not in dbSNP	1,522	1,631
Number of nonsense or essential splice (SNV) variants	16	9
Shared variants	*YAP1* c.370C>T (p.Arg124*)	
	ETFDH c.1093G>T (p.Glu365*)	

Abbreviations are as follows: SNV, single-nucleotide variant; and VCF, variant call format.

variants were detected in any of the known genes associated with eye malformations (all exome sequenced samples had been prescreened for the elimination of those with *SOX2*, *OTX2*, or *PAX6* paired box mutations). Only two shared mutations were detected after filtering on the hypothesis that a rare, clear loss-of-function (LOF) mutation represented the causative variant. One of these was heterozygous nonsense mutation c.1093G>T (p.Glu365*) in *ETFDH* (MIM 231675). Monoallelic LOF mutations in *ETFDH* are not associated with disease phenotypes, whereas the biallelic state causes glutaric acidemia type II (MIM 231680). Given that no other plausible pathogenic *ETFDH* alleles were identified in either individual, we assumed that each is a carrier of this rare autosomal-recessive disease. The other LOF mutation identified was heterozygous nonsense mutation c.370C>T (p.Arg124*) in exon 2 of yes-associated protein 1 (*YAP1* [MIM 606608], RefSeq accession number NM_001130145.2 [canonical transcript variant 1], RefSeq NG_029530.1 [genomic]) (Figure 1). This mutation was present in all four affected individuals in the family and had been inherited from the unaffected grandfather (Figure 1, family 1305 individual I:1). There was no evidence of mosaicism for this apparently nonpenetrant mutation in the peripheral-blood-derived DNA from the grandfather, and no other tissues were available for study. His parents were not available for testing to determine whether he had inherited the mutation. Oligonucleotides used for PCR amplification of *YAP1* are shown in Table S1, available online. No other LOF mutations in *YAP1* were identified in the 700 noncoloboma exomes in the UK10K Rare Diseases Group or in the NHLBI Exome Sequencing Project Exome Variant Server (EVS). The UK10K coloboma exome data (99 exomes, including 75 OFCD-affected individuals from 58 different families) did not contain any missense mutations that were not also present in EVS.

A separate exome sequencing study on ten unrelated individuals with severe bilateral eye malformations identified an individual with a different nonsense mutation in exon 7 of *YAP1*: c.1066G>T (p.Glu356*) (Figure 1, family 132 [abridged affected-only pedigree]). This person has bilateral OFCDs and is part of a large family affected by a previously reported multisystem autosomal-dominant disorder featuring OFCDs, cleft lip with or without cleft palate, intellectual disability, hematuria (without renal impairment or dysplasia), and sensorineural hearing loss (MIM 120433, clinical examination by A.O.M.W.)[16,17] (Table 2). All 13 of the affected family members who were available for testing were found to carry the same nonsense mutation (Figure 1, family132), giving a maximum LOD score of 3.31 at a recombination rate of 0 under the assumption of a maximum allele frequency of 0.0002 (LOD = 3.309 using maximum allele frequency = 0.001). The combined LOD score for the segregation of nonsense mutations in families 1305 and 132 was 4.2. Another family has been reported with a phenotype similar to that of family 132 (family 4, affected by OFCDs and cleft lip and palate).[1] A causative mutation in *YAP1* could not be identified in this family.

On reviewing the array-based comparative genomic hybridization data from 210 individuals with eye malformations, we identified an adult female who has bilateral OFCDs associated with intellectual disability and a large interstitial deletion of 11q (chr11: 84,886,352–113,918,790, clinical examination by A.T.M.). This deletion, which occurred de novo, includes *YAP1* (Figure S1, DECIPHER accession number 282360) in addition to 434 other genes. No other copy-number variants were detected for this region of 11q in the remaining individuals. The association between this deletion and bilateral OFCDs is compatible with the notion that *YAP1* haploinsufficiency is the causative genetic effect. However, no strong conclusion could be drawn in this regard given the large number of other genes in the deleted interval.

Resequencing of *YAP1* in a panel of 336 unrelated OFCD-affected individuals (with no overlap with those sent for exome sequencing) revealed only three rare missense mutations (Figure 1). PCR-based mutation screening analyses were performed as previously described.[7] In family 177, a c.416C>T (p.Pro139Leu) mutation affects a conserved residue that is not associated with a known domain of YAP1 and that is substituted by alanine in data for a *YAP1* allele present in the EVS (Figure S3). The mutation does not segregate with the OFCD phenotype in family 177 (Figure S2). The probands in family 275 (affected by c.988A>G [p.Met330Val]) and family 4162 (affected by c.1385G>A [p.Gly462Glu]) have bilateral OFCDs with microphthalmia and bilateral anophthalmia, respectively. In both cases, there is no family history of eye malformations and no parental samples were available. A single rare missense mutation—c.680C>T (p.Ser227Leu) in family 443—was identified in the UK10K coloboma exome data. This single-nucleotide variant (SNV) was present in 1/13,003 alleles in the EVS (rs376161041). Family 443 is a multiplex consanguineous family, which

Table 2. Clinical Features in Family 132

	Family 132												
	I-2	II-1	II-2	II-3	II-4	III-1	III-2	III-3	III-4	III-5	III-6	III-7	IV-1
Sex	F	F	M	F	F	M	F	F	F	F	M	F	F
Age (years) at last assessment	67	50	49	46	44	28	27	25	24	19	14	12	5
Iris coloboma	Y	Y	Y	Y	?	N	bilateral ectopic pupils	Y	Y	Y	Y	?	Y
Chorioretinal coloboma	Y	Y	?	Y	N	?	Y	Y	Y	Y	N	?	Y
Microphthalmia	Y	N	Y	?	Y	N	Y	N	?	Y	Y	Y	Y
Impaired extraocular muscle function	Y	N	?	?	?	Y	Y	N	?	N	Y	?	Y
Cataract	Y	Y	?	Y	N	N	Y	N	?	N	N	?	N
Cleft palate or cleft uvula	N	N	Y	N	Y	N	N	Y	N	N	Y	Y	N
Cleft lip	N	N	Y	N	Y	N	N	N	N	N	Y	Y	N
Hearing impairment	Y	Y	Y	Y	Y	?	Y	N	Y	Y	Y	Y	?
Learning difficulties	?	?	Y	?	Y	Y	?	?	Y	?	Y	Y	?
Hematuria	N	Y	?	?	Y	N	Y	?	?	Y	?	N	?

Abbreviations are as follows: F, female; N, no; M, male; Y, yes; and ?, unknown.

is compatible with autosomal-recessive inheritance of the eye malformation. No other *YAP1* variant could be identified in the proband, and this SNV did not seem a likely cause of the phenotype in this family. Neither this SNV nor those in families 275 or 4162 change an evolutionarily conserved residue (Figure S3). A custom R script (available upon request) was used for examining the distribution of the rare missense mutations with respect to their position in the open reading frame. The missense mutations identified in the coloboma exome and resequencing data appeared to have a very similar distribution to that of the presumably nonpathogenic missense mutations reported in the EVS (Figure S4). In summary, none of the nonsynonymous variants in the coloboma cohorts can be considered plausible disease-causing variants.

YAP1 encodes transcriptional coactivator YAP1, which, among others, was used in defining the WW domain,[18] found in approximately 100 human gene products. This domain mediates protein-protein interaction via the 4 amino acid proline-rich (PPxY) motif,[18] phosphorylated serine-proline (pSP) motifs,[19] or WW domains of other proteins. There are at least eight splice isoforms of *YAP1*, and each has the potential to encode an altered primary amino acid sequence.[20,21] These can be divided into two groups on the basis of whether the N-terminal half of the protein has one or two WW domains via inclusion or exclusion of coding exon 4. In both groups, there is alternative splicing of coding exon 6 and alternate use of a splice donor site for coding exon 5 (Figure 1).

The canonical role of YAP1 appears to be the major effector of the HIPPO signaling pathway, which is important in the control of organ size during development and is of increasing interest in cancer biology. The subcellular localization of YAP1 and its close homolog, WW-domain-containing transcription regulator 1 (WWTR1, also known as TAZ), is controlled by serine-threonine kinases LATS1 and LATS2 and their modulator, MOB1A, which in turn are regulated by the kinases STK3 and STK4 and their modulator, SAV1. Phosphorylated YAP1 is either retained in the cytoplasm or degraded, whereas nonphosphorylated YAP1 is translocated to the nucleus and functions as a transcriptional coactivator with several different transcription factors, the best studied of which are TEAD1–TEAD4, which mediate the cell-proliferative effects of YAP1.

Complete inactivation of *Yap1* in mice results in developmental arrest at 8.5 days postcoitus (dpc,)[22] leading to multiple system defects, including yolk sac vasculogenesis and embryonic axis elongation. In addition to being involved in HIPPO signaling, YAP1 has also been implicated in the modulation of BMP signaling via interaction with Smad7,[19] WNT signaling via interaction with β-catenin,[23] and NOTCH signaling via upregulation of *JAG1* (MIM 601920).[24] *YAP1* itself is upregulated by hedgehog signaling.[25]

A direct role for *YAP1* in eye development has not previously been identified. To examine site- and stage-specific expression in mouse embryos, we used both whole-mount in situ hybridization with riboprobes targeted to the 3′ UTR of *Yap1* and immunohistochemistry (IHC). This showed expression in the otic vesicle and future brainstem at 9.5 dpc. Expression in the eye was first visible at 10.5 dpc and continued as strong expression on the distal optic cup and overlying surface ectoderm. IHC with the primary antibodies anti-YAP1 (ab56701, Abcam) and anti-PAX2 (PRB-276P, Covance) confirmed this but also suggested that the protein is present in the developing lens and the optic stalk (Figure 2). Using PAX2 as a marker for the optic

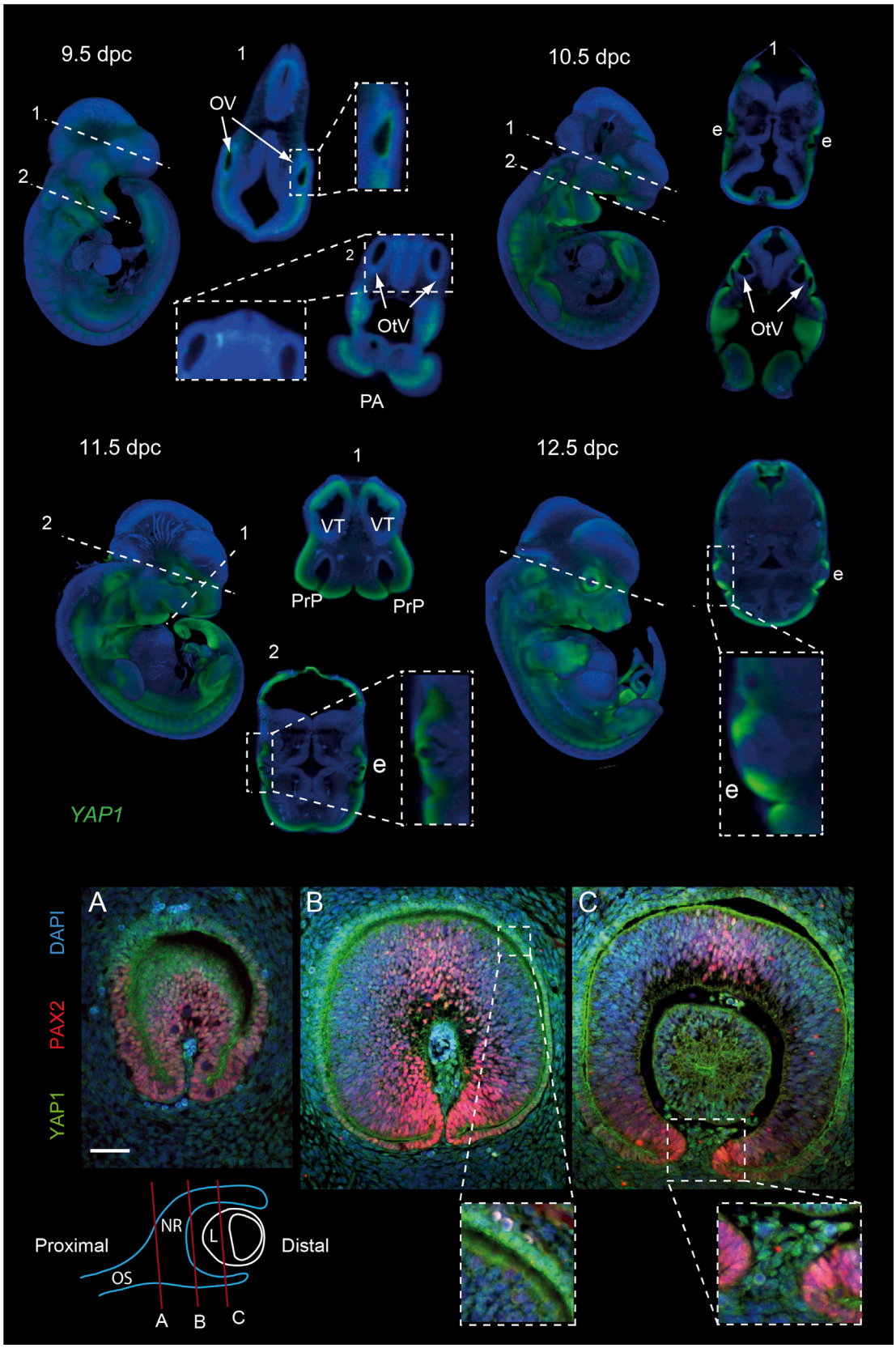

Figure 2. Developmental Expression of YAP1 and *Yap1* during Mouse Development
The top panel shows optical-projection-tomography images of *Yap1* expression detected by whole-mount in situ hybridization on mouse embryos as 9.5, 10.5, 11.5, and 12.5 dpc. At each stage, a 3D reconstruction of the whole embryo is presented on the left. The dashed and numbered white lines indicate the position and angle of the digital sections that are shown to the right of the 3D

(legend continued on next page)

fissure edges, we observed that cells in the periocular mesenchyme (in the gap between the edges) were strongly YAP1 positive. The origin and fate of these interedge cells are not known. Expression was also apparent in the developing brain and in both the maxillary and frontonasal components of the primary palate.

To examine expression in humans, we attempted to quantify *YAP1* in two control lymphoblastoid cell lines (LCLs) and an LCL from the proband in family 132. No cell line was available from any affected member of family 1305. However, *YAP1* expression could not be detected.

One might suspect that these mutations should result in nonsense-mediated decay (NMD) affecting all the reported splice isoforms and thus lead to haploinsufficiency in all tissues. However, this does not explain the clear phenotypic differences between the families. The apparently isolated bilateral OFCD phenotype with one unaffected individual showing complete nonpenetrance in family 1305 contrasted with the broader spectrum of developmental phenotypes in family 132.

A potential explanation for the phenotypic differences between the two families could be *YAP1* expression from an alternative transcriptional start site (TSS). To investigate this possibility, we identified TSSs through genomic mapping of publicly available transcript data from both mouse and human by using spliced expressed sequence tags (ESTs) and cap analysis of gene expression (CAGE) tags.[26] CAGE libraries were constructed with a technique that captures the 5′ ends of 5′ capped mRNAs. The main promoter for *YAP1* strongly and broadly expressed a mean of 33 CAGE tags per million (tpm) and a maximum of 140 tpm. An additional TSS exists in intron 1, and a maximum expression of 1.7 tpm was found in HepG2 cells. This alternative TSS is represented by RefSeq transcript NM_001195045 and supported by at least seven spliced ESTs and a "full-length" mRNA (AK316116). The intron 1 TSS was maximally expressed in carcinoma cell lines but was detected in adult eye-derived tissue samples at >1 per million CAGE tags. The alternative intron 1 TSS was also supported in mouse via multiple spliced ESTs (e.g., CJ167646) and CAGE tags. Mouse expression of this TSS was detected at low levels in multiple tissues and cell types, including adult liver and lung.

We designed RT-PCR assays specific to each TSS (Table S1) and performed reverse transcription by using SuperScript III (Life Technologies). The mouse differs from the human in that it has two different 3′ splice sites in the first exon in the transcripts from the alternative TSS. Amplification from a cDNA template derived from human fetal brain and from mouse embryonic brain, eye, kidney, whole embryo, and various adult tissues showed that both TSSs were used in every developmental and adult tissue examined (Figures 1G and 1I).

To determine whether expression from the alternative TSS could underlie the differences in the phenotypes from the two families, we evaluated where the mutations identified in families 1305 and 132 were located in these transcripts. The position of the nonsense mutation in family 132 was in the coding sequence of all transcripts coming from either TSS. However, the alternative transcript contained the site of the family 1305 nonsense mutation in the 5′ UTR rather than in the coding sequence (Figures 1E and 1F), and it was thus invisible to NMD. Thus, in family 1305, partial rescue of *YAP1* haploinsufficiency by the transcripts from the alternative TSS provides a plausible explanation for the more restricted phenotype. Unfortunately, we were not able to test the differential effect on NMD directly because we did not have access to expressing cell lines or tissues.

However, if such an effect exists, it would suggest that the developing eye is the only tissue that has a dosage-critical requirement for transcripts derived from the canonical TSS. It is not clear why the optic fissure should be particularly sensitive to alteration in YAP1 dosage. The best-studied function of YAP1 is induction of cellular proliferation. Exquisite genetic control of cell growth within the optic vesicle (OV) enables the edges of the optic fissure to appose and subsequently fuse. Reducing YAP1 activity in or around the OV might alter this program of growth to limit or prevent apposition and thus lead to coloboma. Other plausible hypotheses, mentioned above, relate the developmental pathology to noncanonical roles of YAP1 in the SHH and BMP signaling pathways. Further analysis of the site- and stage-specific consequences of *Yap1* loss of function in model organisms is required before any conclusions can be drawn.

Transcripts derived from the alternative TSS have considerable biological interest given that they cannot encode YAP1 with an intact WW1 domain, but they are predicted to encode either a WW2 domain alone or no WW domain at all depending on subsequent alternative splicing. It has recently been shown that both WW1 and WW2 domains are required for YAP1 to bind the Bmp signaling effector Smad1.[19] However, YAP1 with the WW1 domain alone mediates binding of the Bmp signaling inhibitor Smad7.[19] Intriguingly, depletion of Smad7 in mouse embryos results in eye malformation, including coloboma.[27] Given the previous identification of mutations in genes

representation for each stage. The boxed white sections indicate regions that are presented at higher magnification. The abbreviations for the highlighted tissues are as follows: OV, optic vesicle; OtV, otic vesicle; PA, pharyngeal arch; e, eye; PrP, fusing primary palate; and VT, ventral telencephalon. *Yap1* expression is indicated in green. The bottom panel shows immunohistochemical staining of sections from the mouse embryonic eye at 10.5 dpc with antibodies specific to YAP1 (green) and PAX2 (red). Nuclear staining was performed with DAPI. A diagram below indicates the position of the sections along the proximodistal axis of the developing eye. Section A is through the optic stalk (OS); sections B and C both show the neural retina (NR) and lens (L). Higher-magnification images of boxed areas from sections B and C indicate nuclear staining for YAP1 in the RPE and in the periocular mesenchyme between the optic fissure margins, respectively.

encoding BMP signaling molecules and antagonists in human eye malformations,[28–32] it will be important to investigate the effects of YAP1 isoforms with only the WW2 domain on this system.

Supplemental Data

Supplemental Data include four figures and two tables and can be found with this article online at http://www.cell.com/AJHG.

Consortia

Members of the UK10K Rare Diseases Cohorts Working Group are Matthew Hurles (co-chair), David R. FitzPatrick (co-chair), Saeed Al-Turki, Carl Anderson, Inês Barroso, Philip Beales, Jamie Bentham, Shoumo Bhattacharya, Keren Carss, Krishna Chatterjee, Sebhattin Cirak, Catherine Cosgrove, Allan Daly, Jamie Floyd, Chris Franklin, Marta Futema, Steve Humphries, Shane McCarthy, Hannah Mitchison, Francesco Muntoni, Alexandros Onoufriadis, Victoria Parker, Felicity Payne, Vincent Plagnol, Lucy Raymond, David Savage, Peter Scambler, Miriam Schmidts, Robert Semple, Eva Serra, Jim Stalker, Margriet van Kogelenberg, Parthiban Vijayarangakannan, Klaudia Walter, and Gretta Wood.

Acknowledgments

We thank Michael Oldridge, Nicola Ragge, and David Ravine for their assistance with previous analyses of family 132. K.A.W., J.R., M.A., A.M., J.K.R., V.v.H., and D.R.F. are all supported by Medical Research Council (MRC) program grants awarded to the MRC Human Genetics Unit. Funding for UK10K was provided by the Wellcome Trust under award WT091310. We also acknowledge funding from the National Institute of Health Research (Moorfields Eye Hospital Biomedical Research Centre).

Received: November 8, 2013
Accepted: January 2, 2014
Published: January 23, 2014

Web Resources

The URLs for data presented herein are as follows:

1000 Genomes, http://www.1000genomes.org/
DECIPHER, http://decipher.sanger.ac.uk/
FANTOM, http://fantom.gsc.riken.jp/4/
GeneReviews, Lalani, S.R., Hefner, M.A., Belmont, J.W., and Davenport, S.L.H. (1993). CHARGE Syndrome, http://www.ncbi.nlm.nih.gov/books/NBK1117/
NHLBI Exome Sequencing Project (ESP) Exome Variant Server, http://evs.gs.washington.edu/EVS/
Online Mendelian Inheritance in Man (OMIM), http://www.omim.org/
Picard, http://picard.sourceforge.net
RefSeq, http://www.ncbi.nlm.nih.gov/gene/
UCSC Genome Browser, http://genome.ucsc.edu/
UK10K project, http://www.uk10k.org/

Accession Numbers

The DECIPHER accession number for the chromosome 11 deletion reported in this paper is 282360.

References

1. Morrison, D., FitzPatrick, D., Hanson, I., Williamson, K., van Heyningen, V., Fleck, B., Jones, I., Chalmers, J., and Campbell, H. (2002). National study of microphthalmia, anophthalmia, and coloboma (MAC) in Scotland: investigation of genetic aetiology. J. Med. Genet. *39*, 16–22.
2. Chang, L., Blain, D., Bertuzzi, S., and Brooks, B.P. (2006). Uveal coloboma: clinical and basic science update. Curr. Opin. Ophthalmol. *17*, 447–470.
3. Hornby, S.J., Adolph, S., Gilbert, C.E., Dandona, L., and Foster, A. (2000). Visual acuity in children with coloboma: clinical features and a new phenotypic classification system. Ophthalmology *107*, 511–520.
4. Daufenbach, D.R., Ruttum, M.S., Pulido, J.S., and Keech, R.V. (1998). Chorioretinal colobomas in a pediatric population. Ophthalmology *105*, 1455–1458.
5. Mihelec, M., Abraham, P., Gibson, K., Krowka, R., Susman, R., Storen, R., Chen, Y., Donald, J., Tam, P.P., Grigg, J.R., et al. (2009). Novel SOX2 partner-factor domain mutation in a four-generation family. Eur. J. Hum. Genet. *17*, 1417–1422.
6. Wang, P., Liang, X., Yi, J., and Zhang, Q. (2008). Novel SOX2 mutation associated with ocular coloboma in a Chinese family. Arch. Ophthalmol. *126*, 709–713.
7. Gerth-Kahlert, C., Williamson, K., Ansari, M., Rainger, J.K., Hingst, V., Zimmermann, T., Tech, S., Guthoff, R.F., van Heyningen, V., and FitzPatrick, D.R. (2013). Clinical and mutation analysis of 51 probands with anophthalmia and/or severe microphthalmia from a single center. Molecular Genetics & Genomic Medicine *1*, 15–31.
8. Casey, J., Kawaguchi, R., Morrissey, M., Sun, H., McGettigan, P., Nielsen, J.E., Conroy, J., Regan, R., Kenny, E., Cormican, P., et al. (2011). First implication of STRA6 mutations in isolated anophthalmia, microphthalmia, and coloboma: a new dimension to the STRA6 phenotype. Hum. Mutat. *32*, 1417–1426.
9. Schimmenti, L.A., de la Cruz, J., Lewis, R.A., Karkera, J.D., Manligas, G.S., Roessler, E., and Muenke, M. (2003). Novel mutation in sonic hedgehog in non-syndromic colobomatous microphthalmia. Am. J. Med. Genet. A. *116A*, 215–221.
10. Azuma, N., Yamaguchi, Y., Handa, H., Tadokoro, K., Asaka, A., Kawase, E., and Yamada, M. (2003). Mutations of the PAX6 gene detected in patients with a variety of optic-nerve malformations. Am. J. Hum. Genet. *72*, 1565–1570.
11. Kumar, K., Tanwar, M., Naithani, P., Insaan, R., Garg, S., Venkatesh, P., and Dada, R. (2011). PAX6 gene analysis in iridofundal coloboma. Mol. Vis. *17*, 1414–1419.
12. Di Donato, N., Rump, A., Koenig, R., Der Kaloustian, V.M., Halal, F., Sonntag, K., Krause, C., Hackmann, K., Hahn, G., Schrock, E., and Verloes, A. (2013). Severe forms of Baraitser-Winter syndrome are caused by ACTB mutations rather than ACTG1 mutations. Eur. J. Hum. Genet. Published online June 12, 2013.
13. Rivière, J.B., van Bon, B.W., Hoischen, A., Kholmanskikh, S.S., O'Roak, B.J., Gilissen, C., Gijsen, S., Sullivan, C.T., Christian, S.L., Abdul-Rahman, O.A., et al. (2012). De novo mutations in the actin genes ACTB and ACTG1 cause Baraitser-Winter syndrome. Nat. Genet. *44*, 440–444, S1–S2.
14. Wang, L., He, F., Bu, J., Zhen, Y., Liu, X., Du, W., Dong, J., Cooney, J.D., Dubey, S.K., Shi, Y., et al. (2012). ABCB6 mutations cause ocular coloboma. Am. J. Hum. Genet. *90*, 40–48.

15. Olbrich, H., Schmidts, M., Werner, C., Onoufriadis, A., Loges, N.T., Raidt, J., Banki, N.F., Shoemark, A., Burgoyne, T., Al Turki, S., et al.; UK10K Consortium (2012). Recessive HYDIN mutations cause primary ciliary dyskinesia without randomization of left-right body asymmetry. Am. J. Hum. Genet. *91*, 672–684.
16. Kingston, H.M., Harper, P.S., and Jones, P.W. (1982). An autosomal dominant syndrome of uveal colobomata, cleft lip and palate, and mental retardation. J. Med. Genet. *19*, 444–446.
17. Ravine, D., Ragge, N.K., Stephens, D., Oldridge, M., and Wilkie, A.O. (1997). Dominant coloboma-microphthalmos syndrome associated with sensorineural hearing loss, hematuria, and cleft lip/palate. Am. J. Med. Genet. *72*, 227–236.
18. Sudol, M., Bork, P., Einbond, A., Kastury, K., Druck, T., Negrini, M., Huebner, K., and Lehman, D. (1995). Characterization of the mammalian YAP (Yes-associated protein) gene and its role in defining a novel protein module, the WW domain. J. Biol. Chem. *270*, 14733–14741.
19. Aragón, E., Goerner, N., Xi, Q., Gomes, T., Gao, S., Massagué, J., and Macias, M.J. (2012). Structural basis for the versatile interactions of Smad7 with regulator WW domains in TGF-β Pathways. Structure *20*, 1726–1736.
20. Gaffney, C.J., Oka, T., Mazack, V., Hilman, D., Gat, U., Muramatsu, T., Inazawa, J., Golden, A., Carey, D.J., Farooq, A., et al. (2012). Identification, basic characterization and evolutionary analysis of differentially spliced mRNA isoforms of human YAP1 gene. Gene *509*, 215–222.
21. Sudol, M. (2013). YAP1 oncogene and its eight isoforms. Oncogene *32*, 3922.
22. Morin-Kensicki, E.M., Boone, B.N., Howell, M., Stonebraker, J.R., Teed, J., Alb, J.G., Magnuson, T.R., O'Neal, W., and Milgram, S.L. (2006). Defects in yolk sac vasculogenesis, chorioallantoic fusion, and embryonic axis elongation in mice with targeted disruption of Yap65. Mol. Cell. Biol. *26*, 77–87.
23. Rosenbluh, J., Nijhawan, D., Cox, A.G., Li, X., Neal, J.T., Schafer, E.J., Zack, T.I., Wang, X., Tsherniak, A., Schinzel, A.C., et al. (2012). β-Catenin-driven cancers require a YAP1 transcriptional complex for survival and tumorigenesis. Cell *151*, 1457–1473.
24. Tschaharganeh, D.F., Chen, X., Latzko, P., Malz, M., Gaida, M.M., Felix, K., Ladu, S., Singer, S., Pinna, F., Gretz, N., et al. (2013). Yes-associated protein up-regulates Jagged-1 and activates the Notch pathway in human hepatocellular carcinoma. Gastroenterology *144*, 1530, e12.
25. Fernandez-L, A., Northcott, P.A., Dalton, J., Fraga, C., Ellison, D., Angers, S., Taylor, M.D., and Kenney, A.M. (2009). YAP1 is amplified and up-regulated in hedgehog-associated medulloblastomas and mediates Sonic hedgehog-driven neural precursor proliferation. Genes Dev. *23*, 2729–2741.
26. Suzuki, H., Forrest, A.R., van Nimwegen, E., Daub, C.O., Balwierz, P.J., Irvine, K.M., Lassmann, T., Ravasi, T., Hasegawa, Y., de Hoon, M.J., et al.; FANTOM Consortium; Riken Omics Science Center (2009). The transcriptional network that controls growth arrest and differentiation in a human myeloid leukemia cell line. Nat. Genet. *41*, 553–562.
27. Zhang, R., Huang, H., Cao, P., Wang, Z., Chen, Y., and Pan, Y. (2013). Sma- and Mad-related protein 7 (Smad7) is required for embryonic eye development in the mouse. J. Biol. Chem. *288*, 10275–10285.
28. Bakrania, P., Efthymiou, M., Klein, J.C., Salt, A., Bunyan, D.J., Wyatt, A., Ponting, C.P., Martin, A., Williams, S., Lindley, V., et al. (2008). Mutations in BMP4 cause eye, brain, and digit developmental anomalies: overlap between the BMP4 and hedgehog signaling pathways. Am. J. Hum. Genet. *82*, 304–319.
29. Wyatt, A.W., Osborne, R.J., Stewart, H., and Ragge, N.K. (2010). Bone morphogenetic protein 7 (BMP7) mutations are associated with variable ocular, brain, ear, palate, and skeletal anomalies. Hum. Mutat. *31*, 781–787.
30. Okada, I., Hamanoue, H., Terada, K., Tohma, T., Megarbane, A., Chouery, E., Abou-Ghoch, J., Jalkh, N., Cogulu, O., Ozkinay, F., et al. (2011). SMOC1 is essential for ocular and limb development in humans and mice. Am. J. Hum. Genet. *88*, 30–41.
31. Rainger, J., van Beusekom, E., Ramsay, J.K., McKie, L., Al-Gazali, L., Pallotta, R., Saponari, A., Branney, P., Fisher, M., Morrison, H., et al. (2011). Loss of the BMP antagonist, SMOC-1, causes Ophthalmo-acromelic (Waardenburg Anophthalmia) syndrome in humans and mice. PLoS Genet. *7*, e1002114.
32. Kondo, Y., Koshimizu, E., Megarbane, A., Hamanoue, H., Okada, I., Nishiyama, K., Kodera, H., Miyatake, S., Tsurusaki, Y., Nakashima, M., et al. (2013). Whole-exome sequencing identified a homozygous FNBP4 mutation in a family with a condition similar to microphthalmia with limb anomalies. Am. J. Med. Genet. A. *161A*, 1543–1546.